Available online at www.sciencedirect.com
ScienceDirect
Earth and Planetary Science Letters 262 (2007) 620–634
EPSL
www.elsevier.com/locate/epsl

High hydrogen solubility in Al-rich stishovite and water transport in the lower mantle

Konstantin D. Litasov [a,*], Hiroyuki Kagi [b], Anton Shatskiy [c], Eiji Ohtani [a], Dmitry L. Lakshtanov [d], Jay D. Bass [d], Eiji Ito [c]

[a] *Institute of Mineralogy, Petrology and Economic Geology, Tohoku University, Sendai, Japan*
[b] *Geochemical Laboratory, Graduate School of Science, The University of Tokyo, Tokyo, Japan*
[c] *Institute for Study of the Earth's Interior, Okayama University, Misasa, Japan*
[d] *Department of Geology, University of Illinois at Urbana-Champaign, Urbana, USA*

Received 2 March 2007; received in revised form 9 August 2007; accepted 19 August 2007
Available online 24 August 2007
Editor: R.D. van der Hilst

Abstract

Stishovite is an important phase in subducting oceanic crust. The post-garnet assemblage from a precursor eclogite lithology contains up to 25% stishovite at pressures above 25 GPa. This stishovite may contain up to 5 wt.% Al_2O_3. We measured the hydrogen contents of stishovite samples synthesized at 20–25 GPa and 1200–1800 °C from several starting materials containing up to 10 wt.% Al_2O_3. FTIR spectra of stishovite show major bands at 3111–3134 cm^{-1}, with the frequencies increasing as H_2O and Al_2O_3 contents increase, and several minor bands at 2659–2667, 3240, 3261, 3312–3334, and 3351 cm^{-1}. The H_2O content of Al-free stishovite is in the range of 16–30 wt. ppm. The maximum H_2O content of Al-bearing stishovite (4.4 wt.% Al_2O_3) synthesized at 20 GPa and 1400 °C is 3010±300 wt. ppm. Most hydrogen in stishovite is associated with Al^{3+} substitutional defects on the octahedral (Si^{4+}) site. The hydrogen can occupy 40% of vacancies created by incorporation of Al^{3+} at 20 GPa. This observation along with some anomalies in the FTIR spectra may indicate an alternative mechanism of Al^{3+} incorporation into stishovite via the formation of oxygen vacancies or interstitial $Al_i^{\cdot\cdot}$ defects. We report the highest H_2O concentrations in Al-stishovite to date, and argue that it is the most important carrier of water into the lower mantle post-garnet eclogitic assemblages.

Keywords: stishovite; hydrogen; lower mantle; eclogite; infrared spectroscopy

1. Introduction

Recent experimental studies show that water can be transported to the deep lower mantle by hydrous phases (Frost, 1999; Ohtani et al., 2001; Litasov and Ohtani, 2003; Ohtani et al., 2004; Frost, 2006), nominally anhydrous minerals (Bolfan-Casanova et al., 2000; Skogby, 2006; Beran and Libowitzky, 2006; Litasov and Ohtani, in press), and as a fluid captured in disconnected interstitial patches in mantle rocks (Mibe et al., 2003). The role of nominally anhydrous minerals might be most important among these, due to their ability to retain water even at elevated temperatures. Many studies have shown that nominally anhydrous olivine (and its high-pressure modifications wadsleyite and ringwoodite), garnet, and pyroxenes may contain significant amount of structurally bound water, typically

* Corresponding author.
E-mail address: klitasov@ganko.tohoku.ac.jp (K.D. Litasov).

0012-821X/$ - see front matter © 2007 Elsevier B.V. All rights reserved.
doi:10.1016/j.epsl.2007.08.015

as hydroxyl ions (Skogby, 2006; Beran and Libowitzky, 2006; Bell and Rossman, 1992; Kohlstedt et al., 1996; Smyth, 2006).

Most hydrous phases, of which are serpentine, chlorite, clinohumite, chondrodite, and class of so-called dense hydrous magnesium silicates (phases A, E, D, and superhydrous phase B), are stable at low temperatures, corresponding to the cold subducting slabs, and are not stable at normal or ambient mantle temperatures (Litasov and Ohtani, 2003; Litasov and Ohtani, in press; Kawamoto, 2004). Moreover, these phases are stable in a peridotite composition and are not stable in other mantle constituents, such as the eclogite that forms from former oceanic crust. While peridotite comprises the major part of subduction slabs descending into the deep mantle, its degree of hydration is equivocal (e.g. Kerrick, 2002; Rüpke et al., 2004). The part of a subducted slab which is substantially hydrated, at least in 'cold subduction' environments, is oceanic basaltic crust. No hydrous minerals are stable in a typical basaltic composition (eclogite) above 10 GPa (the stability limit of phengite and lawsonite) (e.g. Poli and Schmidt, 1998; Okamoto and Maruyama, 2004; Litasov and Ohtani, 2005). Minor K-amphibole can be stable to 15 GPa (Inoue et al., 1998). Therefore, water can be transported only by the nominally anhydrous minerals of eclogite or by trapped fluids (e.g. Mibe et al., 2003; Ono et al., 2002b). The major minerals in eclogite are garnet, clinopyroxene, and the SiO_2-polymorphs coesite and stishovite. At pressures of 23–28 GPa the garnet-bearing assemblage transforms to a post-garnet assemblage consisting of Al- and Fe-rich Mg-perovskite, Al-rich NAL or CF phases, Ca-perovskite, and stishovite (e.g. Litasov and Ohtani, 2005; Hirose and Fei, 2002; Litasov et al., 2004). Stishovite is one of the most important phases in this lower-mantle post-eclogite assemblage (20–25 modal%).

Pawley et al. (1993) first showed that stishovite, in particular Al-bearing stishovite, can contain significant amounts of water at levels up to 82 wt. ppm H_2O. Thereafter, Chung and Kagi (2002) found up to 844 wt. ppm H_2O in Al-bearing stishovite from eclogite assemblages at 10–15 GPa. The mechanisms of hydrogen incorporation into Al-bearing stishovite were investigated experimentally by Bromiley et al. (2006) and theoretically by Gibbs et al. (2004), leading to the conclusion that H^+ is coupled with Al^{3+} substitutional defects on adjacent octahedral (Si^{4+}) sites. Recently, Lakshtanov et al. (2007b) reported a drastic shift of the post-stishovite transition to $CaCl_2$-structured SiO_2 to lower pressures in Al- and H-bearing system, and argued that Al- and H-bearing stishovite may be responsible for intermittent seismic reflectors observed in the mid-lower mantle (e.g. Le Stunff et al., 1995; Kaneshima and Helffrich, 1999).

In present paper we have determined high water concentrations in stishovite with various Al_2O_3 contents, and argue that the role of stishovite as possible water carrier to the deep mantle might have previously been underestimated.

Table 1
Starting materials for experiments (wt.%)

	SiO_2	TiO_2	Al_2O_3	FeO	MgO	K_2O	H_2O	CO_2
A	94.0		1.0				5.0	
B	92.0		3.0				5.0	
C	87.6		7.4				5.0	
D[a]	87.4		8.2				4.4	
E[a]	84.7		10.0				5.3	
F	59.8				40.2			
G	58.0			7.0	35.0			
H[b]					25.4	29.7	17.1	27.8
I	33.4	1.6	14.4	26.7	18.9		5.0	

[a] H_2O only as $Al(OH)_3$, no distilled H_2O added.
[b] $KHCO_3$–$Mg(OH)_2$ solvent (see Shatskiy et al., in press for details).

2. Experimental procedures

We used several starting compositions to synthesize Al-rich stishovites. The starting materials for the synthesis experiments were pure SiO_2 and Al_2O_3 mixtures with different proportions of the oxides. H_2O was added as $Al(OH)_3$ and as pure distilled H_2O with a total content appropriate for the desired stoichiometry (Table 1). In addition, we used Al-free stishovite crystals from experiments on Mg-perovskite syntheses in the (Mg, Fe)SiO_3–$KHCO_3$–$Mg(OH)_2$ systems (Shatskiy et al., in press). Some data on stishovite compositions and unit cell volumes from perovskite synthesis experiments (Litasov et al., 2003), and high-pressure experiments on MORB compositions (Litasov and Ohtani, 2005; Litasov et al., 2004) were also used for comparison.

The samples were synthesized at 20–26 GPa and 1200–1800 °C using 1000, 1500, and 3000 ton multi-anvil apparatuses installed at Institute of Mineralogy, Petrology and Economic Geology, Tohoku University (Sendai, Japan), and with a 5000 ton multi-anvil apparatus installed at Institute for Study of the Earth's Interior, Okayama University (Misasa, Japan). We used several different cell assemblies for experiments. The details of cell assemblies for truncated edge length of the WC anvils (TEL) of 2.0 and 3.5 mm can be found in (Litasov and Ohtani, 2002), and those for TEL = 6.0 mm can be found in (Shatskiy et al., in press). We used ZrO_2

and MgO pressure media and $LaCrO_3$ heaters. All samples were sealed in welded Pt capsules. Temperature was monitored by $W_{97\%}Re_{3\%}$–$W_{75\%}Re_{25\%}$ thermocouples. Pressure was calibrated using the semiconductor-to-metal transitions in ZnS, GaAs, and GaP at room temperature, and using the olivine–wadsleyite, wadsleyite–ringwoodite, and ringwoodite = Mg-perovskite + periclase transitions in Mg_2SiO_4 (Morishima et al., 1994; Suzuki et al., 2000; Katsura et al., 2003; Katsura et al., 2004; Fei et al., 2004) for TEL 3.5 and 6.0 mm, and using in situ synchrotron experimental data (e.g. Litasov et al., 2004; Litasov et al., 2005) for TEL 2.0 mm.

After recovering the sample capsules, they were cut close to the middle by a diamond saw. The smaller part was mounted into epoxy and polished for electron microprobe analyses, whereas single crystals or polycrystalline aggregates from the larger part were separated from the Pt capsule and used for Fourier transform infrared (FTIR) measurements.

The chemical composition of stishovite and melt were determined by an electron microprobe (JEOL Superprobe JXA-8800) at Tohoku University. An accelerating voltage of 15 kV and 10 nA specimen current were used for the analyses. Volume data were obtained using microfocus X-ray powder diffractometer (MacScience M18XCE) at Tohoku University. The orientation of single-crystal sample plates and unit cell volumes were measured by angle-dispersive X-ray diffractometry (ADX), using a Bruker 4-circle diffractometer with a CCD detector at the University of Illinois (Lakshtanov et al., 2007a,b).

Polarized infrared spectra were obtained using a micro-FTIR spectrometer (Spectrum 2000, Perkins Elmer Co Ltd.) at the University of Tokyo. IR measurements were carried out using a Globar light source, KBr beam-splitter and MCT detector. The polarized spectra were obtained on optically clear single crystals, which were double polished according to the crystallographic orientation (see Chung and Kagi, 2002 for further details). Additionally, unpolarized infrared spectra of polycrystalline samples were obtained using a Jasco MFT-2000 micro-FTIR spectrometer at Tohoku University. Measurements were carried out using a tungsten light source, a Ge-coated KBr beam-splitter and a high sensitivity, wide-band MCT detector. Several hundred scans were accumulated for each spectrum with 1 cm^{-1} resolution and 50 or 100 μm apertures. Background corrections of absorbance spectra were carried out by a spline fit of the baseline defined by points outside the OH-stretching region (Litasov et al., 2003).

Micro-FTIR spectra were measured for double-polished thin sections of polycrystalline aggregates or single-crystal stishovite placed on a single-crystal diamond (artificial type IIa diamond, Sumitomo) or KBr plate. The thickness of the thin sections and separate single crystals were varied from 8–20 μm for samples with the highest Al_2O_3 and H_2O contents, up to 100–200 μm for samples with low Al_2O_3 contents and

Table 2
Experimental details and H_2O contents of stishovite

Sample	Starting material	*P*, Gpa	*T*, °C	Time, min	Assemblage	*V*, Å^3	Al_2O_3 (wt.%)	H_2O, wt. ppm		Remarks
								(Paterson, 1982)	(Pawley et al., 1993)	
K-328	A	20	1800	120	St+L	46.53 (3)	0.10 (2)	146 (15)	90 (8)	P — 25 [a]
K-329	A	20	1800	120	St+L	46.55 (2)	0.25 (7)	175 (33)	108 (20)	S — 60
K-341	B	20	1800	120	St+L	46.74 (2)	1.40 (12)	354 (87)	217 (60)	S — 60
K-342	B	20	1800	120	St+L	46.84 (2)	1.92 (33)	609 (160)	375 (100)	P — 40
K-323	C	25	1400	300	St+L	47.01 (3)	3.28 (21)	1711 (550)	1060 (330)	P — 30
K-322	C	25	1800	60	St+L	47.09 (4)	3.63 (26)	1290 (420)	740 (240)	P — 30
K-325	C	20	1400	300	St+Egg+L	47.21 (1)	4.36 (12)	3010 (300)	1840 (180)	S — 150
K-324	C	20	1800	60	St+L	47.64 (1)	6.07 (5)	2380 (200)	1475 (130)	S — 350
K-359	D	20	1200	300	St+Egg+L	47.21 (6)	4.48 (38)	2900 (350)	1790 (210)	S — 120
K-355	D	20	1700	120	St+L	47.72 (5)	7.62 (30)	2610 (300)	1600 (200)	S — 200
K-343	E	20	1800	120	St+L	47.36 (3)	4.80 (13)	1007 (280)	631 (170)	P — 30
K-285	E	20	1800	60	St+L	47.38 (5)	5.13 (46)	2150 (500)	1330 (300)	P — 40
A-745	FH	20	1600	60	St+L	46.46 (2)	0.00	16 (3)	8 (2)	S — 400
A-794	FH	24	1750	60	St+L	46.49 (2)	0.00	31 (3)	17 (2)	S — 500
A-810 [b]	GH	24	1500	90	St+MgPv+L	46.47 (1)	0.00	38 (5)	21 (3)	S — 200
K-161 [b]	I	26	1200	900	St+MgPv+L	46.93 (5)	2.10 (30)	618 (260)	373 (170)	S — 60

S, single crystal; P, polycrystalline aggregate.
One standard deviation of analyses and measurements is shown in parenthesis and is related to last mentioned digits.
[a] Maximum size of the crystals in μm.
[b] Fe_2O_3 contents of stishovites are as follows (wt.%): A-810 = 0.07 (4); K-161 = 0.59.

Al-free stishovite. The H_2O contents were determined by the method of Paterson (1982) where absorption bands were integrated by using the calibration of the extinction coefficient and density factors calculated similarly to those of Bolfan-Casanova et al. (2000):

$$C_{OH} = \frac{X_i}{150\xi}\int \frac{K(\overline{v})}{(3780-\overline{v})}d\overline{v}$$

where C_{OH} is the concentration of hydroxyl (in H/10^6Si or wt. ppm H_2O), ξ is an orientation factor, and $K(\overline{v})$ is the absorption coefficient in cm^{-1} for a given wavenumber $\overline{v}$. X_i is a density factor, which can be calculated as $X_i = 18/2d \times 10^6$ (if C_{OH} is in wt. ppm H_2O) and $X_i = M/d \times 10^6$ (if C_{OH} is in H/10^6Si). Here d is the mineral density (in g/l) and M is the molar mass (in g/mol). Additionally, we calculated H_2O contents using calibration by Pawley et al. (1993):

$$C_{OH} = \frac{A}{l} \times \frac{M_{SiO2} \times 10^6}{d} \cdot \frac{1}{I}$$

where C_{OH} is the concentration of hydroxyl (in H/10^6Si), A is the integrated absorbance of the OH-stretching vibration, l is thickness of the sample, M_{SiO2} is molecular weight of SiO_2, d is density of the mineral, and I is the integrated molar absorption coefficient of the vibration ($I = 163{,}000 \pm 120{,}000$ liter cm^{-2} mol^{-1}). Since the error in estimating an absorption coefficient in the latter calibration is large, we used the H_2O contents calculated by Paterson's (1982) calibration for discussion in this paper.

3. Results

It should be noted that hydrogen is incorporated into stishovite as a hydroxyl ion (OH^-), which is observed in FTIR spectra. However, for simplicity and consistency with previous studies we express hydrogen/hydroxyl contents of stishovite in ppm H_2O by weight, which can be simply recalculated to wt. ppm hydroxyl or H/10^6Si contents.

The experimental P–T conditions, compositions, and H_2O contents of the stishovite samples are listed in Table 2. The sizes of the stishovite crystals were typically 100–150 μm, whereas the largest crystals were up to 500 μm. In some samples we observed only fine-grained polycrystalline aggregates of 10–40 μm crystals (Table 2, Fig. A1, *see online version of this paper*).

In all experiments the Al_2O_3 content of stishovite was less than the Al_2O_3 content of the starting material.

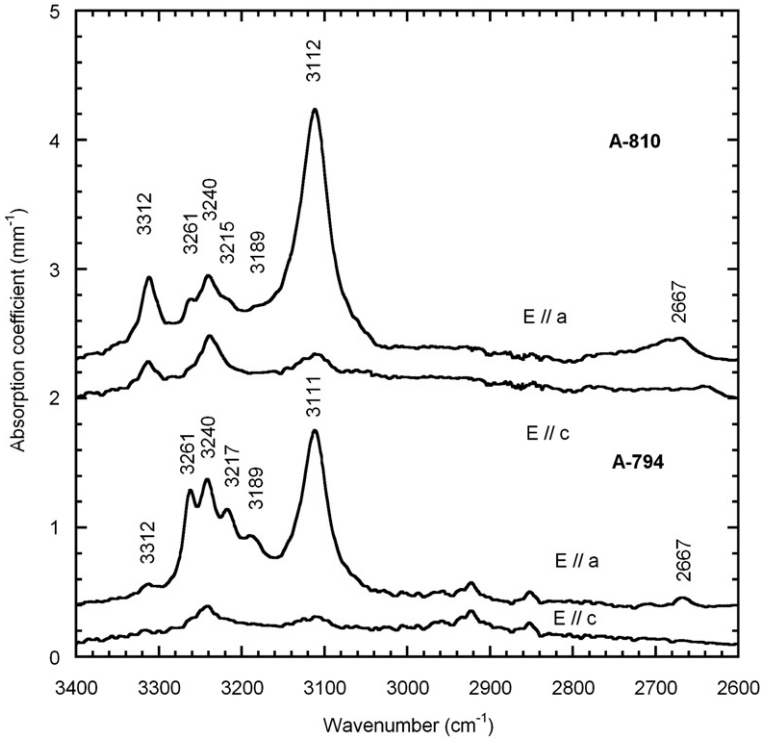

Fig. 1. Polarized FTIR spectra of Al-free stishovite (Sample A-794, 24 GPa, 1750 °C) and Al-free stishovite containing 0.1 wt.% FeO (Sample A-810, 24 GPa, 1500 °C).

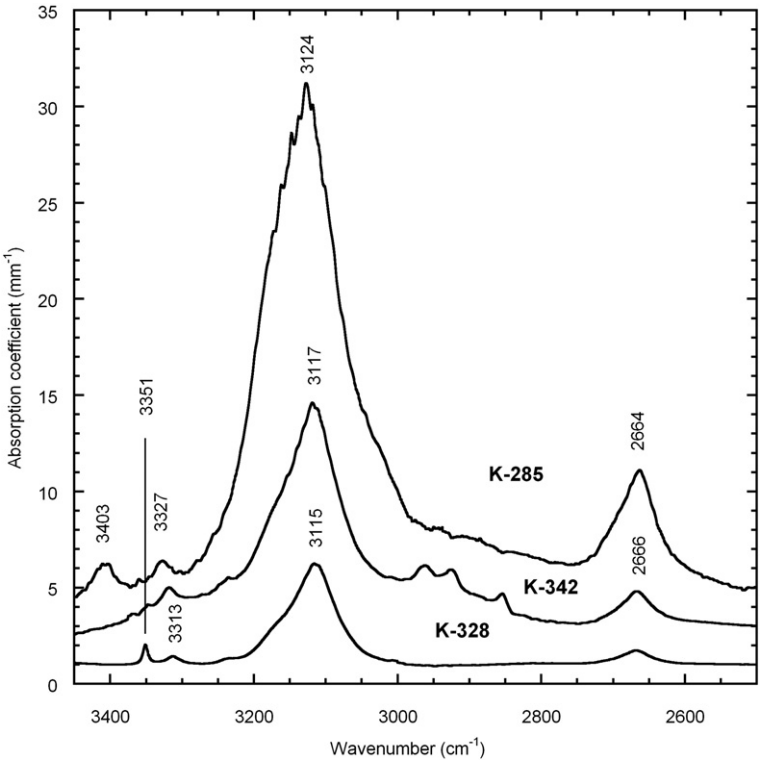

Fig. 2. Unpolarized FTIR spectra of polycrystalline Al-bearing stishovite.

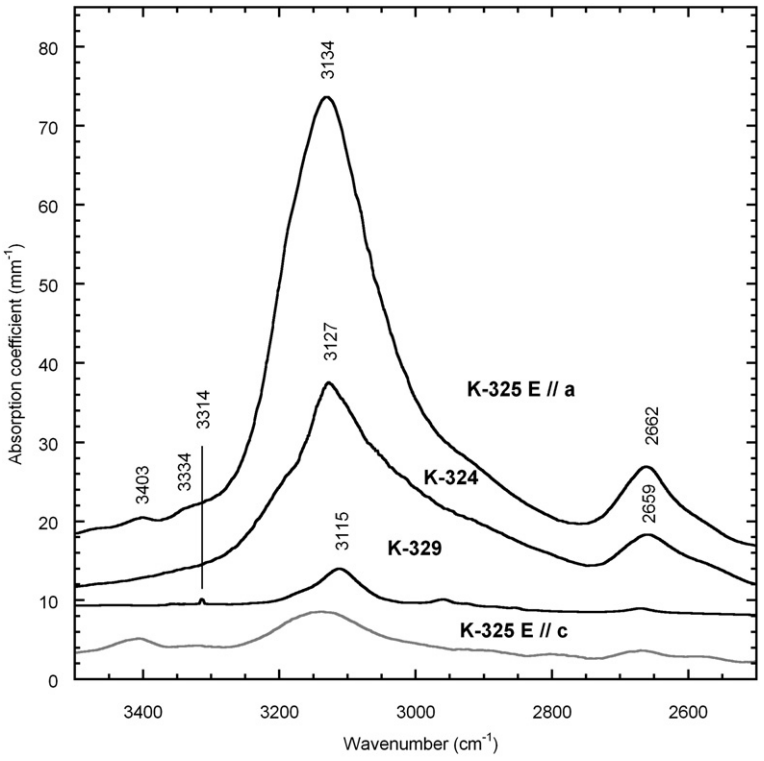

Fig. 3. Polarized FTIR spectra of Al-bearing stishovite.

Table 3
Positions of major OH-absorption bands (cm^{-1}) in stishovites with different Al_2O_3 contents

Sample	Al_2O_3, wt.%	1	2	3	4	5	6	7
A-745	0	2667	3111		3240	3261	3312	3351
A-794	0	2667	3111	3217	3240	3261	3312	
A-810	0[a]	2667	3112	3215	3240	3261	3312	
K-328	0.10	2667	3115		3240		3313	3351
K-329	0.25	2667	3115		3240		3314	
K-342	1.92	2666	3117				3318	
K-325	4.36	2662	3134				3334	
K-359	4.48	2662	3132				3331	
K-343	4.80	2663	3120				3322	
K-324	6.07	2659	3127					
K-355	7.62	2656	3130					

[a] Fe_2O_3=0.07 wt.%.

However, we do not observe corundum in the run products, indicating the preferential partitioning of Al_2O_3 to a hydrous melt. Electron microprobe analyses of the melt phases indicate that the partition coefficient of Al_2O_3 between stishovite and melt ($D^{St/melt}_{Al2O3}$) varies from 0.1 to 0.6 (Table A1, *see online version of this paper*). We did not observe the partial melt in the samples K-322 and K-323 synthesized at 25 GPa. However it is likely that partial melts are present in these samples, because we do not observe corundum, and excess of Al_2O_3 (Table 1) must be accommodated in the partial melt.

Phase Egg was observed in two run at 20 GPa and 1200–1400 °C (Fig. A1, *see online version of this paper)*, which is consistent with its stability field (Ono, 1999; Sano et al., 2004). Maximum Al_2O_3 contents (6.1–7.6 wt.%) were measured in stishovite synthesized at 1700–1800 °C and 20 GPa. The Al_2O_3 contents of stishovite synthesized at 25 GPa are lower than those at 20 GPa (Table 2).

Representative FTIR spectra of stishovite are shown in Figs. 1–3. The spectra of Al-free stishovite contain OH absorption bands at 2667, 3111, 3189, 3217, 3240, 3261 and 3312 cm^{-1} (Fig. 1). Spectra of sample A-745 also contain a minor band at 3351 cm^{-1}. All bands except one at 3240 cm^{-1} are observed to be highly anisotropic and have vibration directions perpendicular to *c* axis. Al- and Fe-free stishovite contains 16–31 wt. ppm H_2O. IR spectra and the H_2O content of stishovite containing minor Fe (most likely as Fe^{3+}) are comparable to those for pure stishovite (Fig. 1).

The IR spectra of Al-bearing stishovites contain one major broad and asymmetrical absorption band at 3111–3134 cm^{-1} and some additional bands, which are generally similar to those for Al-free stishovites. The positions of bands at 3111 and 3312 cm^{-1}, observed in spectra of Al-free stishovites, are significantly shifted toward higher frequencies with increasing Al_2O_3 and H_2O contents (Figs. 2–3, Table 3). Maximum shifts to 3134 and 3334 cm^{-1}, respectively, were observed in spectra of stishovite containing 4.4 wt.% Al_2O_3 and the highest H_2O content (3010 wt. ppm H_2O), but not in those for stishovite with the highest Al_2O_3 content (6.1–7.2 wt.%). The position of the band at 2667 cm^{-1} shifts to lower frequencies with increasing Al_2O_3 content in stishovite.

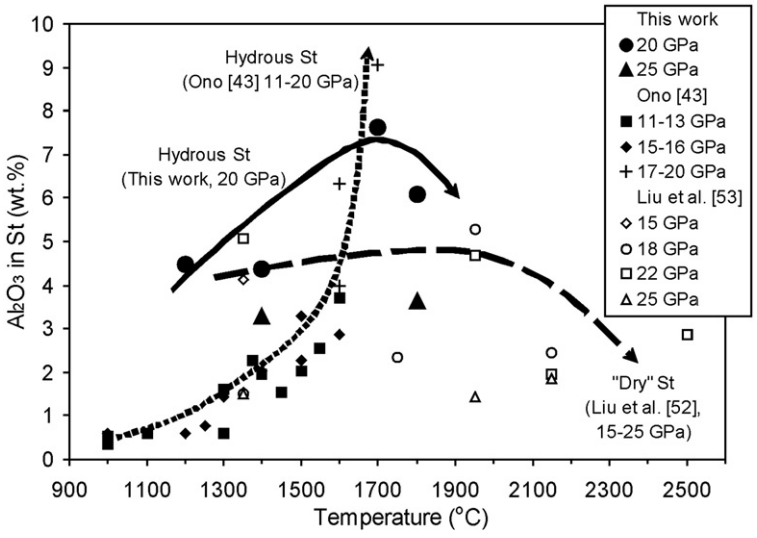

Fig. 4. Temperature dependence of Al_2O_3 contents of stishovite at 11–25 GPa. Arrows show general trends of Al_2O_3 versus temperature according to different studies.

This band was not reported previously for stishovite; however, its intensity is consistent with that of a major band at 3111–3134 cm^{-1}, indicating that it is connected with the vibration of structurally bonded OH. An additional band can be recognized at 3160–3180 cm^{-1}, which appears as a shoulder on the main band (Figs. 2–3). However, the exact position of this band is poorly constrained. This band was also observed by Bromiley et al. (2006).

Three minor peaks at 2850–2950 cm^{-1} are related to CH_3-groups, which appear to be due to contamination from acetone or bond material (typically these bands cannot be removed by drying and heating of the sample in an oven).

The variations of Al_2O_3 and H_2O contents in our stishovites are not completely systematic, which may indicate hydrogen loss through the Pt capsule in some experiments. This may change the H_2O content of the melt coexisting with stishovite and, therefore, leads to a decrease of the H_2O content of stishovite according to the stishovite/melt partition coefficient for H_2O. The hydrogen loss in some experiments correlates with the size of the crystals. The H_2O content is typically higher in coarse-grained single-crystal stishovite, and lower in fine-grained aggregates. A similar tendency is observed for Al_2O_3, which is suggestive of a direct relationship between Al_2O_3 and H_2O incorporation in stishovite. However, the data indicate a general tendency for Al_2O_3 to increase with temperature (with a possible maximum at 1700 °C) and to decrease with pressure (in the pressure interval of 20–25 GPa) (Fig. 4). Accordingly, H_2O contents decreases with temperature and pressure at 20–25 GPa, while mostly depends on Al_2O_3 content of stishovite.

Fig. 5 shows that the unit cell volume of stishovite changes linearly as a function of Al_2O_3 content. Hydrogen incorporation appears to have a minor effect compared to that of Al_2O_3, because samples with different H_2O contents do not deviate significantly from the major trend of the data in Fig. 5. The observed volume increase is consistent with data for stishovites reported previously (Smyth et al., 1995; Ono et al., 2002c; Lakshtanov et al., 2005) and those observed in dry and hydrous MORB (Litasov and Ohtani, 2005 and our unpubl. data). The deviation of MORB-stishovites to higher volumes may be with a result of the incorporation of minor Fe_2O_3 and other impurities, which would increase the unit cell volumes.

4. Discussion

4.1. Solubility of hydrogen and aluminium in stishovite

H_2O contents of pure stishovite measured at 20 GPa and 1600 °C and 24 GPa and 1750 °C are 16 and 31 wt. ppm, respectively. This is slightly higher relative to values obtained previously (7 wt. ppm at 10 GPa and 1200 °C (Pawley et al., 1993); 3 wt. ppm at 15 GPa and 1500 °C

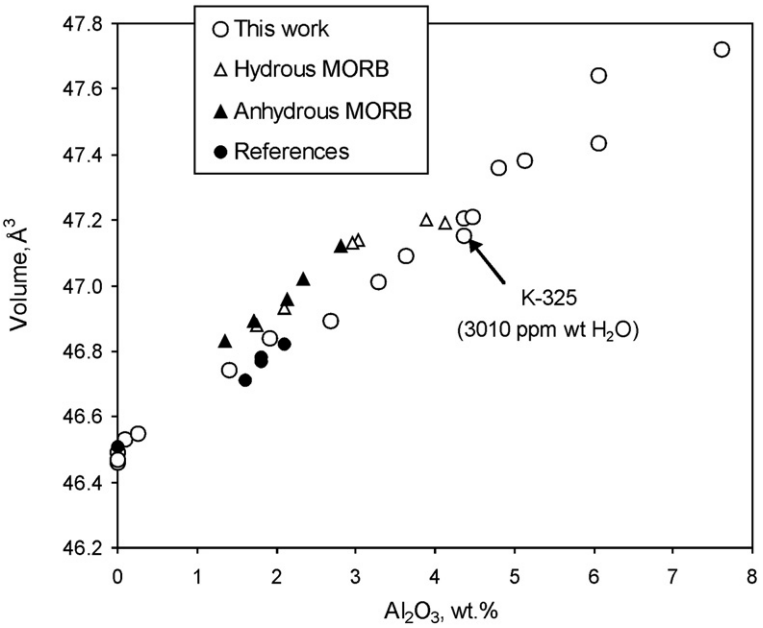

Fig. 5. Unit cell volume of Al- and H-bearing stishovites as a function of Al_2O_3 content. Data for hydrous and anhydrous MORB is from (Litasov and Ohtani, 2005). Note that MORB-stishovites contain trace amounts of Fe_2O_3. Reference data are from Smyth et al., 1995; Ono et al., 2002c; Lakshtanov et al., 2005.

(Bromiley et al., 2006), and is similar to those reported by Bolfan-Casanova et al. (2000) (15–72 wt. ppm in stishovite synthesized at 15–21 GPa and 1200–1500 °C). High H_2O concentrations (72 wt. ppm) in pure stishovite reported in (Bolfan-Casanova et al., 2000) are unlikely and may be due to the presence of minor impurities of trivalent cations in the starting material (Bromiley et al., 2006; Mosenfelder, 2000) (see also Section 4.2.).

The maximum H_2O contents of Al-bearing stishovite were measured, on samples synthesized at 20 GPa and 1400 °C, is 3010 wt. ppm. This value is almost 4 times higher than previously reported H_2O concentrations in Al-stishovite (844 wt. ppm, Chung and Kagi, 2002). It is also consistent with the theoretically calculated maximum H_2O content of Al-stishovite (3000 wt. ppm H_2O at 25 GPa 1223 °C Panero and Stixrude, 2004), although the theoretical models of Panero and Stixrude (2004) assumed the incorporation of Al and H in a 1:1 ratio. H_2O (as well as Al_2O_3) contents in samples K-325 (3010 wt. ppm) and K-359 (2900 wt. ppm) can be considered as at the solubility limit (which some would take as the "true solubility") of H_2O in stishovite at these conditions, since stishovite coexists with phase Egg and melt. According to Keppler and Bolfan-Casanova (2006), the solubility of H_2O in a mineral at the supercritical conditions (at pressures and temperatures beyond the second critical endpoint) can be defined in the invariant assemblage (for example, three phases, stishovite+melt+phase Egg, in the three-component system), where the H_2O content in a phase depends only on pressure and temperature. In other runs stishovite coexists with melt only and its H_2O contents depend on H_2O contents of the coexisting melt, thus representing a lower limit on the maximum H_2O solubility.

It was also argued that H_2O contents increase with increasing pressure and temperature (Panero and Stixrude, 2004; Panero et al., 2003). In the present experiments we observed a decrease of H_2O contents with increasing temperature, but it may be related to the experimental temperatures (1200–1800 °C) being in a range where the H_2O contents decreases with increasing proportion of partial melt (e.g. Smyth et al., 2006). At lower temperatures, corresponding to the subducting slabs (1000–1200 °C at 20–25 GPa), a positive correlation of H_2O content with temperature (when it is controlled mainly by incorporation of Al_2O_3) is possible. We have found that H_2O contents depends significantly on the activity of H_2O in the system. If the size of the crystals in the recovered sample is small, indicating hydrogen loss during experiment, the H_2O contents of stishovite are systematically lower than those in large single crystals of coarse-grained samples. Consequently, it is difficult to suggest a pressure dependence of H_2O contents in stishovite from our experiments, since all runs at 25 GPa contain fine-grained polycrystalline stishovite and no visible melt.

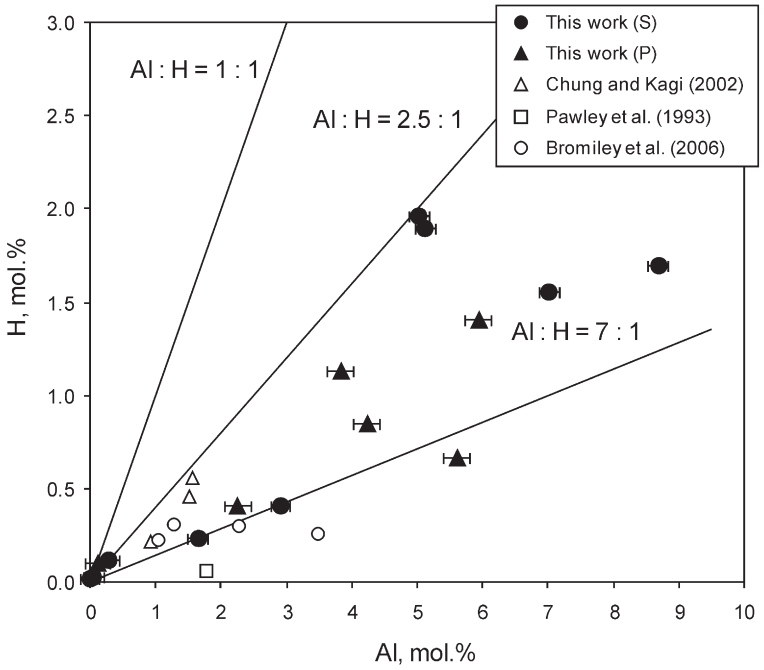

Fig. 6. Incorporation of H^+ into stishovite as a function of Al^{3+} content. S, single crystal; P, polycrystalline stishovite.

The H_2O contents of stishovite are strongly correlated with Al_2O_3 (Fig. 6). Bromiley et al. (2006) noted that H_2O contents in stishovite reaches a maximum at around 1–2 wt.% Al_2O_3 and then decreases, which may be connected with a different mechanism of Al_2O_3 incorporation into stishovite at 15 GPa (see Section 4.2). However, we have shown that significantly more hydrogen can be incorporated in stishovite with high Al_2O_3 contents at 20 GPa (Fig. 6).

The Al_2O_3 incorporation in stishovite observed in present study is generally consistent with data reported in Liu et al. (2006). These authors observed a significant increase of Al_2O_3 contents in stishovite with temperature, with a maximum near 1700–1800 °C followed by a gradual decrease in Al_2O_3 content at higher temperatures (Fig. 4). This trend is in broad agreement with previous data on hydrous ASH-system (Ono, 1999) and dry and hydrous MORB systems (Litasov and Ohtani, 2005; Hirose and Fei, 2002; Yasuda et al., 1994). At the same time, Al_2O_3 contents of stishovite from hydrous MORB systems are notably higher relative to those from anhydrous systems (Litasov and Ohtani, 2005).

The pressure dependence of Al_2O_3 contents in stishovite is not clear. Liu et al. (2006) observed a decrease of Al_2O_3 contents in anhydrous stishovite in the pressure range 14–25 GPa. However, Ono (1999) observed nearly the same Al_2O_3 contents in hydrous stishovite in the pressure range of 11–20 GPa. The data for anhydrous and hydrous MORB indicate that Al_2O_3 contents in stishovite increase with pressure at 10–28 GPa (from 0.5 to 4.0 wt.% near solidus temperatures (Litasov and Ohtani, 2005; Hirose and Fei, 2002; Yasuda et al., 1994; Ono et al., 2001); however, in this case Al_2O_3 content strongly depends on the composition of the coexisting Al-rich phases (garnet in the transition zone and Al-rich NAL and CF phases and Mg-perovskite in the lower mantle; see Section 4.3). Ono (1999) reported a maximum Al_2O_3 content (~9 wt.%) in hydrous stishovite synthesized at 20 GPa and 1700 °C. Panero and Stixrude (2004) also argued that the Al_2O_3 content in stishovite increases with pressure, which is consistent with some diamond anvil cell results showing 8–14 wt.% Al_2O_3 in stishovite (or post-stishovite phases ?) at 25–60 GPa (Kesson et al., 1994; Miyajima et al., 1999).

4.2. Mechanism for hydrogen and aluminium incorporation in stishovite

The mechanisms of hydrogen and aluminium incorporation in stishovite are considered in details by Bromiley et al. (2006) and our data are generally consistent with their results.

The major mechanism for hydrogen incorporation in stishovite is related to the presence of the absorption band at 3111–3134 cm^{-1}, which has a >95% component of vibration perpendicular to the *c* axis. Bromiley et al. (2006) argued that this is consistent with the hydrogen incorporation mechanism proposed in Smyth et al. (1995), where H is located close to one of the shared O–O edges in the plane of an $O–Si_3$ triangle. However, Gibbs et al. (2004) argued that this band may be connected with H positioned nearly perpendicular to that proposed in Smyth et al. (1995), in the same plane perpendicular to the *c* axis (see Fig. 1 in Gibbs et al., 2004), which is energetically favourable according to their theoretical calculations for Al-bearing stishovite. The shift of the OH band at 3111 cm^{-1} to higher frequencies with increasing H_2O and Al_2O_3 contents, is consistent with increasing the volume and distortion of octahedra by substitution of Si^{4+} by Al^{3+}. An O–H stretching frequency of 3111–3134 cm^{-1} corresponds to moderate-to-strong H bonding (Libowitzky, 1999), in accordance with both of the above mentioned models. Bromiley et al. (2006) observed an additional band at 3158–3167 cm^{-1} as a shoulder on the main band at 3111–3117 cm^{-1}. In our spectra the band at 3158–3167 (3160–3180) cm^{-1} is poorly recognized; however we can see asymmetrical shape and minor shoulder in this region in the spectra of Al-bearing stishovites (Figs. 2–3). Accordingly, they argued that peaks at 3111–3134 cm^{-1} and 3160–3180 cm^{-1} may reflect different H positions relative to the octahedral site, corresponding to: (a) mechanisms proposed in Smyth et al. (1995) or Gibbs et al. (2004) (coupled Al^{3+} H^{+} substitution); and (b) H docking adjacent to an AlO_6 octahedron.

The band at 3111–3134 cm^{-1} is present in the spectra of the both Al-free and Al-bearing stishovite, indicating that hydrogen can be associated with an octahedral vacancy without charge balancing by Al^{3+}. At the same time, it was noted that nominally Al-free stishovite may contain 8.2 wt. ppm Al according to manufacturer data on the purity of SiO_2 (Alfa-Aesar) (Bromiley et al., 2006), and therefore a few wt. ppm H_2O in stishovite can indeed be charge balanced by minor impurities of trivalent cations in starting oxide reagents.

The band at 3312–3334 cm^{-1} shows an almost identical shift relative to the band at 3111–3134 cm^{-1}, while its intensity exhibits different behavior, being more pronounced in stishovites with low Al_2O_3 contents. This 3312–3334 cm^{-1} band may correspond to vibration of an O–H bond towards one of the large interstitial sites in the structure, similarly to the mechanism proposed for minor OH bands in rutile (Bromiley

et al., 2006; Koudriachova et al., 2004; Bromiley and Shiryaev, 2006). It remains associated with a trivalent cation on the adjacent octahedral site, which is consistent with its synchronized vibration with the major band at 3111–3134 cm^{-1}.

The assignment of additional OH band in all stishovite spectra at 2659–2667 cm^{-1}, which was not observed in previous studies, is more problematic. This band has the same anisotropy as the major band at 3111–3134 cm^{-1}. However, it shifts slightly in the opposite direction to the major band; that is, to lower frequencies from 2667 cm^{-1} in Al-free stishovite to 2659 cm^{-1} in Al-bearing stishovite.

The spectra of Al-free stishovite or stishovite with low Al_2O_3 contents also contain OH bands at 3217, 3240, 3261, and 3351 cm^{-1}. The positions of these bands do not change with increasing Al_2O_3 content and have markedly different anisotropies than the main band at 3111–3134 cm^{-1}. Therefore, they can be related to different mechanisms of hydrogen incorporation. According to Bromiley et al. (2006), who also observed al least one of these bands at 3238 cm^{-1}, these bands could be related to interstitial H associated with minor Si^{4+} vacancies in the octahedral sites.

As shown in Fig. 6, probably less than 1/2 of the Al atoms are charge balanced with hydrogen to satisfy the electro-neutrality conditions in the stishovite we studied. Al^{3+} incorporation in stishovite can be charge balanced by two mechanisms (Bromiley et al., 2006; Hirose et al., 2005). Firstly, by the formation of an oxygen vacancy:

$$2Si_{Si}^{x} + O_{O}^{x} + (Al_2O_3) \rightarrow 2Al_{Si}^{\prime} + \ddot{V}_{O} + 2(SiO_2) \qquad (1)$$

A second mechanism is the coupled substitution of Al^{3+} onto the large, distorted octahedral interstitial site in the stishovite structure, which is most probable at highest pressures:

$$3Si_{Si}^{x} + 2(Al_2O_3) \rightarrow 3Al_{Si}^{\prime} + Al_{i}^{\cdots} + 3(SiO_2) \qquad (2)$$

Most Al should be incorporated by mechanism (1) (Smyth et al., 1995) with vacancies, which can be coupled further with hydrogen. However, Bromiley et al. (2006) suggested that mechanism (2) might be also important, because they observed maximum in hydrogen solubility at 1–2 wt.% Al_2O_3 in stishovite and a decrease of hydrogen contents at higher Al_2O_3 contents. It was shown that mechanism (2) might be important in reduced rutile (when Ti^{4+} is substituted by Ti^{3+}) and be responsible for its blue colour (Khomenko et al., 1998), Al-bearing rutile (Gesenhues and Rentschler, 1999), and the high-pressure α-PbO_2–SiO_2 phase, containing 12 wt.% Al_2O_3 (Hirose et al., 2005).

The incorporation of Al into stishovite increases the volume of the stishovite unit cell (Lakshtanov et al., 2005, 2007a) and increases it nearly linearly (Fig. 5). According to Gibbs et al. (2004), the difference in volume between AlO_6 and SiO_6 octahedron is ~10%. Assuming this same effect on the volume change, the incorporation of 4.2 mol.% Al^{3+} coupled with H^{+} could produce ~0.4% volume increase (Gibbs et al., 2004; Panero and Stixrude, 2004). Although this 0.4% value for the volume is likely a maximum (the unit cell volume change will be less than the octahedral volume change), in fact it is less than half of the volume change measured in this study (~1.3% for 4.2 mol.% Al^{3+}, or 3.6 wt.% Al_2O_3) (Fig. 5). Al incorporation by mechanism (1) only, implies that on a per mole basis, the effect of oxygen vacancies on the volume of stishovite is ~5 times greater than that of hydrogen defects (Lakshtanov et al., 2005, 2007a) and may explain increase of the unit cell volume of Al-stishovite. However, the presence of $Al_i^{\cdots}$ defects can be suggested from differences in frequencies of major OH bands in spectra of stishovite, containing 4.4 wt.% Al_2O_3 and 3010 wt. ppm H_2O (sample K-325), and those of stishovite, containing 6.1 wt.% Al_2O_3 and 2380 wt. ppm H_2O (sample K-324). In the latter spectra, position of major band are shifted to lower frequencies (3127 cm^{-1} and 3134 cm^{-1}, respectively), which oppose to general trend for the samples with lower Al_2O_3 contents (Table 3). Similar explanation was proposed in Bromiley et al. (2006), however the shift of the position of major OH band in opposite direction was less pronounced. It is obvious that Al incorporation into stishovite by mechanism (2) would decrease the hydrogen solubility and change octahedral volumes and O–O distances compared with Al incorporated by mechanism (1).

4.3. Stishovite as a water carrier in the lower mantle

As was noted above, the major portion of a subducted slab which is substantially hydrated and which will not be dehydrated, at least in 'cold subduction' environments, is oceanic basaltic crust. In addition, stishovite may be a major phase within the uppermost sediment layer of a subducting slab which, however, is relatively thin and may not contribute in a major way to the water budget of the deep mantle.

Lawsonite and phengite are stable up to 10 GPa and about 1000 °C in basaltic compositions (Poli and Schmidt, 1998). At higher pressures water can be stored in the nominally anhydrous phases of eclogite (Fig. 7).

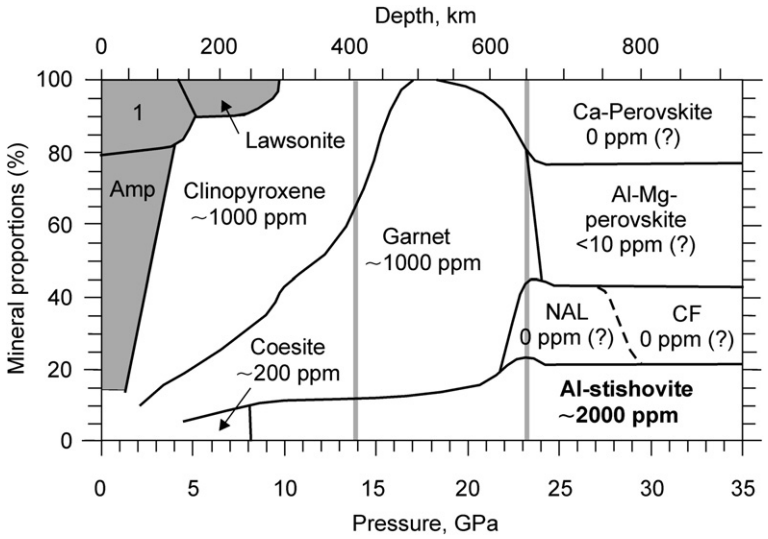

Fig. 7. Mineral proportions and water contents in minerals (in wt. ppm H_2O) of hydrous oceanic crust (eclogite) along a subduction slab geotherm, after (Litasov and Ohtani, in press). The field labelled 1 is a multiphase field including chlorite, epidote, staurolite, chloritoid, zoisite and some other phases. Other abbreviations: Amp, amphibole; NAL; Na–Al phase; CF, Al-rich Ca-ferrite-structured phase.

The major minerals in eclogite are garnet, clinopyroxene, and the SiO_2-polymorphs coesite and stishovite. Clinopyroxene (including omphacite and jadeite) can store a significant amount of water (up to 1000 wt. ppm H_2O; e.g. Koch-Müller et al., 2004). Maximum concentrations may exceed 3000 wt. ppm as reported for omphacite from ultrahigh-pressure eclogites of the Kokchetav massif, Kazakhstan (Katayama and Nakashima, 2003). However, clinopyroxene is dissolved in garnet with pressure and is not stable above 15–20 GPa (Okamoto and Maruyama, 2004; Litasov and Ohtani, 2005). Data for the solubility of H_2O in pyrope garnet are relatively controversial. Ackermann et al. (1983) and Geiger et al. (1991) reported 200–700 wt. ppm H_2O in pyrope synthesized at 2–5 GPa and 800–1200 °C. In the experiments at 1000 °C it was found that the water contents in pyrope increases with pressure from 73 wt. ppm at 1.5 GPa to 199 wt. ppm at 10 GPa (Lu and Keppler, 1997). Xia et al. (2005) reported high concentrations of H_2O in pyrope-almandine garnet from ultrahigh-pressure eclogites of Dabieshan (China). The concentrations ranged from 92 to 1735 wt. ppm and are heterogeneously distributed at 1 cm scale. The data on water contents in majoritic garnet are limited. Bolfan-Casanova et al. (2000) measured 677 wt. ppm H_2O in $MgSiO_3$ tetragonal garnet and Katayama et al. (2003) reported 1130–1250°wt. ppm H_2O in majorite related to the basaltic systems. These data indicate that nominally anhydrous eclogite assemblage of upper mantle and transition zone can accommodate up to 1000 wt. ppm H_2O as structurally bound hydrogen. It should be noted also that hydrous fluid can be trapped in eclogite and transported to the deep mantle in amounts up to 1–2 wt.%, since it has a high dihedral angles, $\theta = 62–68^{o}$ (at 3–5 GPa and 700–800 °C) in a pyroxene/garnet matrix (Mibe et al., 2003; Ono et al., 2002b).

At pressures of 23–28 GPa, the garnet-bearing assemblage transforms to a post-garnet assemblage consisting of Al- and Fe-rich Mg-perovskite, Al-rich NAL (Na–Al) or CF (Ca-ferrite-structured) phase, Ca-perovskite and stishovite (Fig. 7) (e.g. Litasov and Ohtani, 2005; Hirose and Fei, 2002; Litasov et al., 2004). Stishovite, being less abundant at transition zone pressures (8–10 modal%), becomes one of the most important phase of post-eclogite assemblage in the lower mantle (20–25 modal%). None of the phases in this assemblage was reported to contain significant amounts of H_2O. Potentially, Al- and Fe-bearing Mg-perovskite and Al-bearing Ca-perovskite can contain significant amounts of H_2O due to vacant substitution in Si-site (e.g. Navrotsky, 1999). However, experimental data on water contents in silicate perovskites indicate that it is very low and does not exceed 10–50 wt. ppm H_2O (Litasov et al., 2003; Bolfan-Casanova et al., 2003). It is important to emphasize that OH bands were observed in Al- and Fe-bearing Mg-perovskite at high pressures, as suggested by synchrotron IR measurements (Reid et al., 2006), indicating that debates on water in Mg-perovskite are not finished. We would suggest, however, that it is not likely that Mg-perovskite (including Al- and Fe-bearing sample) can accommodate more than 100–200 wt. ppm H_2O. Hydrogen contents in $CaSiO_3$-

perovskites unknown, because it is amorphous at low pressures. Yet, FTIR spectra of Al-bearing $CaGeO_3$-perovskite, synthesized at 15 GPa and 1300–1900 °C, do not contain visible OH absorption bands (our unpubl. data). Preliminary studies indicate that FTIR spectra of CF and NAL Al-phases also do not contain OH absorption bands (Litasov and Ohtani, 2004).

The Al_2O_3 contents (or total $Al_2O_3+Cr_2O_3+Fe_2O_3$) of stishovite in eclogitic assemblage may exceed 4.0 wt.% (e.g. Litasov and Ohtani, 2005; Ono et al., 2001). The maximum Al_2O_3 content of stishovite (5.0 wt.%) in the MORB system at 27 GPa and 1500 °C were reported in Irifune and Ringwood (1993). Consequently, Al-bearing stishovite can be considered as the most important hydrogen-bearing phase in lower mantle post-garnet assemblage.

4.4. Hydrogen and aluminium in stishovite and post-stishovite phase transitions

There have been several reports of local and semi-global seismic discontinuities and heterogeneities in the depth range of 1000–1600 km (e.g. Le Stunff et al., 1995; Kaneshima and Helffrich, 1999). For example, a dipping low-velocity layer in the vicinity of the Mariana and Izu–Bonin subduction zones at depth of 1400–1600 km was reported in Kaneshima and Helffrich (1999). Similarly, a reflector at ~1200 km in a different tectonic setting was observed by Le Stunff et al. (1995). A phase transition is SiO_2 was considered to be important in explaining these seismic reflectors.

Stishovite is the lowest-pressure SiO_2 polymorph with octahedrally coordinated silicon. At ~50–55 GPa and 25 °C it undergoes a second order Landau-type phase transition to the orthorhombic $CaCl_2$ structure (Pnnm) (e.g. Kingma et al., 1995; Andrault et al., 1998). Ono et al. (2002a) reported data at high temperature and suggested that the stishovite to $CaCl_2$–SiO_2 transformation occurs at ~75 GPa and 1500 °C, assuming an approximate $dT/dP=0.012$ K/GPa. However, the Clapeyron slope of this reaction was poorly constrained from experiments. Theoretical calculations suggest a more modest slope of $dT/dP=0.004$ K/GPa (Kingma et al., 1995). Therefore, it was argued that the post-stishovite transition cannot be responsible for mid-lower mantle seismic reflectors (e.g. Ono et al., 2002a).

Recently, Lakshtanov et al. (2007b) observed that the post-stishovite phase transition in Al- and H-bearing system (sample K-324, containing 6.1 wt.% Al_2O_3) occurs at 25 GPa and 25 °C, i.e. the pressure of the post-stishovite transition decreases dramatically with the addition of aluminium and hydrogen. Assuming a linear dependence of the transition pressure on Al content and a $dP/dT=0.004$ GPa/K, we can estimate a lower bound of ~36 GPa for the pressure at which this phase transition would occur along a mantle geotherm, corresponding to depth of ~950 km (Lakshtanov et al., 2007). As a result, a shift of the post-stishovite phase boundary to lower pressures may be very important for explaining seismic reflectors in the mid-lower mantle, since only a few vol.% of stishovite is needed to cause a visible seismic discontinuity (Karki et al., 1997).

Hirose et al. (2005) reported Al-stishovite (3.4 wt.% Al_2O_3) to be stable at 60 GPa and ~1900 °C in a MORB-type composition, which is broadly consistent with observations by Lakshtanov et al. (2007b) and indicates a significant shift of the post-stishovite phase boundary (~20 GPa) to lower pressures even in an anhydrous system relative to pure SiO_2 (Ono et al., 2002a). To our knowledge, there are no reports on the Al_2O_3 contents of $CaCl_2$–SiO_2. Further phase transformations of the $CaCl_2$–SiO_2 phase to the α-PbO_2–SiO_2 phase was observed at 121 GPa and 2123 °C (Murakami et al., 2003). However, in the MORB system this transformation occured at 110 GPa at same temperature (Hirose et al., 2005). The Al_2O_3 content of α-PbO_2–SiO_2 phase at 113 GPa is 12.6 wt.% (Hirose et al., 2005).

Hydrogen incorporation into $CaCl_2$–SiO_2 and α-PbO_2–SiO_2 phases remains enigmatic. The hydrogen contents in Fe-bearing TiO_2 (II) phase, isostructural to α-PbO_2–SiO_2 was found to be zero at 6–7 GPa and 1100 °C (Bromiley et al., 2004). It should be noted that the pressure of the rutile to TiO_2 (II) phase transition in theFe-bearing TiO_2 system was found to be significantly lower compared with the transition pressure for pure TiO_2 (Bromiley et al., 2004; Withers et al., 2003). A similar effect is observed for the $CaCl_2$–SiO_2 to α-PbO_2–SiO_2 phase transition with addition of Al_2O_3 (Hirose et al., 2005; Murakami et al., 2003).

5. Conclusions

1. We measured hydrogen contents in stishovite synthesized at 20–25 GPa and 1200–1800 °C from several starting materials containing up to 10 wt.% Al_2O_3. FTIR spectra of stishovite show major bands at 3111–3134 cm^{-1}, with the frequencies increasing as H_2O and Al_2O_3 content increases (to a maximum observed Al_2O_3 content of 7.62 wt.%), and several minor bands at 2659–2667, 3240, 3261, 3312–3334, and 3351 cm^{-1}.
2. The H_2O contents of Al-free stishovite were 16–30 wt. ppm. The maximum H_2O content of Al-bearing stishovite (4.4 wt.% Al_2O_3) synthesized at 20 GPa and 1400 °C is 3010±300 wt. ppm. Most hydrogen in

stishovite is associated with Al^{3+} substitutional defects on the octahedral (Si^{4+}) site. However, only 1/2.5 to 1/4 (25–40%) of the vacancies created by incorporation of Al^{3+} are associated with H^{+}. This observation may indicate an alternative mechanism of Al^{3+} incorporation into stishovite via formation of oxygen vacancies or interstitial $Al_i^{\cdot\cdot}$ defects.

3. The H_2O contents expected in Al-bearing stishovite (1000–2000 wt. ppm H_2O) from eclogite in upper mantle and transition zone assemblages is comparable with those of majorite and clinopyroxene (1000 wt. ppm H_2O). However, in a post-garnet assemblage that would be stable in the lower mantle and composed of Al- and Fe-rich Mg-perovskite + Al-rich NAL or CF phase + Al-stishovite, + Ca-perovskite, stishovite is most important water carrier.
4. The Al_2O_3 contents of stishovite are higher in hydrous systems. Thus, hydrogen may further induce a dramatic shift of the post-stishovite phase transition to lower pressures, in which Al_2O_3 plays a dominant role. Accordingly, Al- and H-bearing stishovite can be responsible for mid-mantle seismic reflectors in the depth range of 1000–1600 km (Lakshtanov et al., 2007b).

Acknowledgements

We thank two anonymous reviewers for helpful comments. This work was conducted as a part of the 21st Century Center-of-Excellence program at Tohoku and Okayama Universities and supported by the grants in Aid for Scientific Researches from the Ministry of Education, Culture, Sports, Science and Technology, Japan (Nos 14102009 and 16075202) to EO and a grant in Aid for young scientists from Japanese Society for Promotion of Science (No 17740344) to KDL. Support was also provided by the US National Science Foundation under grants EAR 0135642 and 0003383 (to JDB).

Appendix A. Supplementary data

Supplementary data associated with this article can be found, in the online version, at doi:10.1016/j.epsl.2007.08.015.

References

Ackermann, L., Cemic, L., Langer, K., 1983. Hydrogarnet substitution in pyrope: a possible location for "water" in the mantle. Earth Planet. Sci. Lett. 62, 208–214.

Andrault, D., Fiquet, G., Guyot, F., Hanfland, M., 1998. Pressure-induced Landau-type transition in stishovite. Science 282, 720–724.

Bell, D.R., Rossman, G.R., 1992. Water in Earth's mantle: the role of nominally anhydrous minerals. Science 255, 1391–1397.

Beran, A., Libowitzky, E., 2006. Water in natural mantle minerals II: olivine, garnet, and accessory minerals. In: Keppler, H., Smyth, J.R. (Eds.), Water in Nominally Anhydrous Minerals. Rev. Mineral. Geochem. 62, pp. 169–191.

Bolfan-Casanova, N., Keppler, H., Rubie, D.C., 2000. Water partitioning between nominally anhydrous minerals in the MgO–SiO_2–H_2O system up to 24 GPa: implications for the distribution of water in the Earth's mantle. Earth Planet. Sci. Lett. 182, 209–221.

Bolfan-Casanova, N., Keppler, H., Rubie, D.C., 2003. Water partitioning at 660 km depth and evidence for very low water solubility in magnesium silicate perovskite. Geophys. Res. Lett. 30. doi:10.1029/2003GL017182.

Bromiley, G.D., Bromiley, F.A., Bromiley, D.W., 2006. On the mechanism for H and Al incorporation in stishovite. Phys. Chem. Miner. 33, 613–621.

Bromiley, G.D., Hilaret, N., McCammon, C., 2004. Solubility of hydrogen and ferric iron in rutile and TiO_2 (II): implications for phase assemblages during ultrahigh-pressure metamorphism and for stability of silica polymorphs in the lower mantle. Geophys. Res. Lett. 31, L04610. doi:10.1029/2004GL.019430.

Bromiley, G.D., Shiryaev, A., 2006. Neutron irradiation and post-irradiation annealing of rutile (TiO_2-x): effect on hydrogen incorporation and optical absorption. Phys. Chem. Miner. 33, 426–434.

Chung, J.I., Kagi, H., 2002. High concentration of water in stishovite in the MORB system. Geophys. Res. Lett. 29, 2020. doi:10.1029/2002GL015579.

Fei, Y., Van Orman, J., Li, J., van Westrenen, W., Sanloup, C., Minarik, W., Hirose, K., Komabayashi, T., Walter, M., Funakoshi, K., 2004. Experimentally determined postspinel transformation boundary in Mg_2SiO_4 using MgO as an internal pressure standard and its geophysical implications. J. Geophys. Res. 109. doi:10.1029/2003JB002562.

Frost, D.J., 1999. The stability of dense hydrous magnesium silicates in Earth's transition zone and lower mantle. In: Fei, Y., Bertka, C.M., Mysen, B.O. (Eds.), Mantle Petrology: field observations and high pressure experimentation: A tribute to F.R. Boyd. Geochem. Soc. Spec. Publ., 6, pp. 283–296.

Frost, D.J., 2006. The stability of hydrous mantle phases. In: Keppler, H., Smyth, J.R. (Eds.), Water in Nominally Anhydrous Minerals. Rev. Mineral. Geochem. 62, pp. 243–271.

Geiger, C.A., Langer, K., Bell, D.R., Rossman, G.R., Winkler, B., 1991. The OH^{-} component in synthetic pyrope. Am. Mineral. 76, 49–59.

Gesenhues, U., Rentschler, T., 1999. Crystal growth and defect structure of Al^{3+} — doped rutile. J. Solid State. Chem. 143, 210–218.

Gibbs, G.V., Cox, D.F., Ross, N.L., 2004. A modelling of the structure and favourable H-doking sites and defects for the high-pressure silica polymorph stishovite. Phys. Chem. Miner. 31, 232–239.

Hirose, K., Fei, Y., 2002. Subsolidus and melting phase relations of basaltic composition in the uppermost lower mantle. Geochim. Cosmochim. Acta 66, 2099–2108.

Hirose, K., Takafuji, N., Sata, N., Ohishi, Y., 2005. Phase transition and density of subducted MORB crust in the lower mantle. Earth Planet. Sci. Lett. 237, 239–251.

Inoue, T., Irifune, T., Yurimoto, H., Miyagi, I., 1998. Decomposition of K-amphibole at high pressures and implications for subduction zone volcanism. Phys. Earth Planet. Inter. 107, 221–231.

Irifune, T., Ringwood, A.E., 1993. Phase transformations in subducted oceanic crust and buoyancy relationships at depths of 600–800 km in the mantle. Earth Planet. Sci. Lett. 117, 101–110.

Kaneshima, S., Helffrich, G., 1999. Dipping low–velocity layer in the mid-lower mantle: evidence for geochemical heterogeneity. Science 283, 1888–1891.

Karki, B.B., Stixrude, L., Crain, J., 1997. Ab initio elasticity of three high-pressure polymorphs of silica. Geophys. Res. Lett. 24, 3269–3272.

Katayama, I., Nakashima, S., 2003. Hydroxyl in clinopyroxene from the deep subducted crust: evidence for H_2O transport into the mantle. Am. Mineral. 88, 229–234.

Katayama, I., Hirose, K., Yurimoto, H., Nakashima, S., 2003. Water solubility in majoritic garnet in subduction oceanic crust. Geophys. Res. Lett. 30. doi:10.1029/2003GL018127.

Katsura, T., Yamada, H., Nishikawa, O., Song, M., Kubo, A., Shinmei, T., Yokoshi, S., Aizawa, Y., Yoshino, T., Walter, M.J., Ito, E., Funakoshi, K., 2004. Olivine–wadsleyite transition in the system (Mg,Fe)2SiO4. J. Geophys. Res. 109, B02209. doi:10.1029/2003JB002438.

Katsura, T., Yamada, H., Shinmei, T., Kubo, A., Ono, S., Kanzaki, M., Yoneda, A., Walter, M.J., Ito, E., Urakawa, S., Funakoshi, K., Utsumi, W., 2003. Post-spinel transition in Mg_2SiO_4 determined by high P–T *in situ* X-ray diffraction. Phys. Earth Planet. Inter. 136, 11–24.

Kawamoto, T., 2004. Hydrous phase stability and partial melt chemistry in H_2O-saturated KLB-1 peridotite up to the uppermost lower mantle conditions. Phys. Earth Planet. Inter. 143–144, 387–395.

Keppler, H., Bolfan-Casanova, N., 2006. Thermodynamics of water solubility and partitioning. Rev. Miner. Geochem. 62, 193–230.

Kerrick, D., 2002. Serpentine seduction. Science 298, 1344–1345.

Kesson, S., FitzGerald, J.D., Shelley, J.M.G., 1994. Mineral chemistry and density of subducted basaltic crust at lower mantle pressures. Nature 372, 767–769.

Khomenko, V., Langer, K., Rager, H., Fett, A., 1998. Electronic absorption by Ti^{3+} ions and electronic delocalization in synthetic blue rutile. Phys. Chem. Miner. 25, 338–346.

Kingma, K.J., Cohen, R.E., Hemley, R.J., Mao, H.K., 1995. Transformation of stishovite to a denser phase at lower mantle pressures. Nature 374, 243–245.

Koch-Müller, M., Matsyuk, S.S., Wirth, R., 2004. Hydroxyl in omphacites and omphacitic clinopyroxenes of upper mantle to lower crustal origin beneath the Siberian platform. Am. Mineral. 89, 921–931.

Kohlstedt, D.L., Keppler, H., Rubie, D.C., 1996. Solubility of water in the α, β, and γ phases of $(Mg,Fe)_2SiO_4$. Contrib. Mineral. Petrol. 123, 345–357.

Koudriachova, M., de Leeuw, S., Harrison, N., 2004. First-principles study of H intercalation in rutile TiO_2. Phys. Rev. B 70, 165421.

Lakshtanov, D.L., Litasov, K.D., Sinogeikin, S.V., Hellwig, H., Li, J., Ohtani, E., Bass, J.D., 2007a. Effect of Al^{3+} and H^+ on the elastic properties of stishovite. Am. Mineral. 92, 1026–1030.

Lakshtanov, D.L., Sinogeikin, S.V., Litasov, K.D., Prakapenka, V.B., Hellwig, H., Wang, J., Sanches-Valle, C., Perrillat, J.P., Chen, B., Somayazulu, M., Li, J., Ohtani, E., Bass, J.D., 2007b. The poststishovite phase transition in hydrous alumina-bearing SiO_2 in the lower mantle of the Earth. Proc. National Acad. Sci. 104, 13588–13590. doi:10.1073/pnas.0706113104.

Lakshtanov, D.L., Vanpeteghem, C.B., Jackson, J.M., Bass, J.D., Shen, G.Y., Prakapenka, V.B., Litasov, K.D., Ohtani, E., 2005. The equation of state of Al,H-bearing SiO_2 stishovite to 58 GPa. Phys. Chem. Miner. 32, 466–470.

Le Stunff, Y., Wicks, C.W., Romanowicz, B., 1995. P′p′ precursors under Africa — evidence for mid-mantle reflectors. Science 270, 74–77.

Libowitzky, E., 1999. Correlation of O–H stretching frequencies and O–H···O hydrogen bond lengths in minerals. Monatsh. Chem. 130, 1047–1059.

Litasov, K.D., Ohtani, E., in press. Effect of water on the phase relations in the Earth's mantle and deep water cycle, *in* "Advances in High-Pressure Mineralogy", E. Ohtani ed., Geol. Soc. Amer. Spec. Paper, 421.

Litasov, K.D., Ohtani, E., Langenhorst, F., Yurimoto, H., Kubo, T., Kondo, T., 2003. Water solubility in Mg-perovskites and water storage capacity in the lower mantle. Earth Planet. Sci. Lett. 211, 189–203.

Litasov, K.D., Ohtani, E., 2002. Phase relations and melt compositions in CMAS-pyrolite–H_2O system up to 25 GPa. Phys. Earth Planet. Inter. 134, 105–127.

Litasov, K.D., Ohtani, E., 2005. Phase relations in hydrous MORB at 18–28 GPa: implications for heterogeneity of the lower mantle. Phys. Earth Planet. Inter. 150, 239–263.

Litasov, K.D., Ohtani, E., 2004. Relationship of the Al-bearing phases NAL and CF in the lower mantle. Russ. Geol. Geophys. 45, 1313–1325.

Litasov, K.D., Ohtani, E., Sano, A., Suzuki, A., Funakoshi, K., 2005. *In situ* X-ray diffraction study of post-spinel transformation in a peridotite mantle: implication to the 660-km discontinuity. Earth Planet. Sci. Lett. 238, 311–328.

Litasov, K.D., Ohtani, E., 2003. Stability of various hydrous phases in CMAS pyrolite–H_2O system up to 25 GPa. Phys. Chem. Miner. 30, 147–156.

Litasov, K.D., Ohtani, E., Suzuki, A., Kawazoe, T., Funakoshi, K., 2004. Absence of density crossover between basalt and peridotite in the cold slabs passing through 660 km discontinuity. Geophys. Res. Lett. 31. doi:10.1029/2004GL021306.

Liu, X., Nishiyama, N., Sanehira, T., Inoue, T., Higo, Y., Sakamoto, S., 2006. Decomposition of kyanite and solubility of Al_2O_3 in stishovite at high pressure and high temperature conditions. Phys. Chem. Miner. 33, 711–721.

Lu, R., Keppler, H., 1997. Water solubility in pyrope to 100 kbar. Contr. Miner. Petrol. 129, 35–42.

Mibe, K., Yoshino, T., Ono, S., Yasuda, A., Fujii, T., 2003. Connectivity of aqueous fluid in eclogite and its implications for fluid migration in the Earth's interior. J. Geophys. Res. 108, 2295. doi:10.1029/2002JB001960.

Miyajima, N., Fujino, K., Funamori, N., Kondo, T., Yagi, T., 1999. Garnet–perovskite transformation under conditions of the Earth's lower mantle: an analytical transmission electron microscopy study. Phys. Earth Planet Inter. 116, 117–131.

Morishima, H., Kato, T., Suto, M., Ohtani, E., Urakawa, S., Utsumi, W., Shimomura, O., Kikegawa, T., 1994. The phase boundary between α-and β-Mg_2SiO_4 determined by in situ X-ray observation. Science 265, 1202–1203.

Mosenfelder, J.L., 2000. Pressure dependence of hydroxyl solubility in coesite. Phys. Chem. Miner. 27, 610–617.

Murakami, M., Hirose, K., Ono, S., Ohishi, Y., 2003. Stability of $CaCl_2$-type and α-PbO_2-type SiO_2 at high pressure and temperature determined by in situ X-ray measurements. Geophys. Res. Lett. 30, 1207. doi:10.1029/2002GL016722.

Navrotsky, A., 1999. Mantle geochemistry: a lesson from ceramics. Science 284, 1788.

Ohtani, E., Litasov, K., Hosoya, T., Kubo, T., Kondo, T., 2004. Water transport into the deep mantle and formation of a hydrous transition zone. Phys. Earth Planet. Inter. 143–144, 255–269.

Ohtani, E., Touma, M., Litasov, K., Kubo, T., Suzuki, A., 2001. Stability of hydrous phases and water storage capacity in the

transitional zone and lower mantle. Phys. Earth Planet. Inter. 124, 105–117.

Okamoto, K., Maruyama, S., 2004. The eclogite–garnetite transformation in the MORB + H_2O system. Phys. Earth Planet. Inter. 146, 283–296.

Ono, S., 1999. High temperature stability limit of phase egg, $AlSiO_3$ (OH). Contr. Miner. Petrol. 137, 83–89.

Ono, S., Ito, E., Katsura, T., 2001. Mineralogy of subducted basaltic crust (MORB) from 25 to 37 GPa and chemical heterogeneity of the lower mantle. Earth Planet. Sci. Lett. 190, 57–63.

Ono, S., Hirose, K., Murakami, M., Isshiki, M., 2002a. Post-stishovite phase boundary in SiO_2 determined by in situ X-ray observations. Earth Planet. Sci. Lett. 197, 187–192.

Ono, S., Mibe, K., Yoshino, T., 2002b. Aqueous fluid connectivity in pyrope aggregates: water transport into the deep mantle by a subducted oceanic crust without any hydrous minerals. Earth Planet. Sci. Lett. 203, 895–903.

Ono, S., Suto, T., Hirose, K., Kuwayama, Y., Komabayashi, T., Kikegawa, T., 2002c. Equation of state of Al-bearing stishovite to 40 GPa at 300 K. Am. Mineral. 87, 1486–1489.

Panero, W.R., Benedetti, L.R., Jeanloz, R., 2003. Transport of water into lower mantle: role of stishovite. J. Geophys. Res. 108. doi:10.1029/2002JB002053.

Panero, W.R., Stixrude, L.P., 2004. Hydrogen incorporation in stishovite at high pressure and symmetric bonding in δ-AlOOH. Earth. Planet. Sci. Lett. 221, 421–431.

Paterson, M.S., 1982. The determination of hydroxyl by infrared absorption in quartz, silicate glasses and similar materials. Bull. Mineral. 105, 20–29.

Pawley, A., McMillan, P.F., Holloway, J.R., 1993. Hydrogen in stishovite, with implications for mantle water content. Science 261, 1024–1026.

Poli, S., Schmidt, M.W., 1998. The high pressure stability of zoisite and phase relations of zoisite-bearing assemblages. Contr. Miner. Petrol. 130, 162–175.

Reid, F.R., Jacobsen, S.D., Watson, H.C., Liu, Z., Lin, J., Langenhorst, F., Demouchy, S., Smyth, J.R., Fei, Y., Hemley, R., Mao, H., 2006. Synthesis and high-pressure synchrotron-infrared studies of OH-bearing silicate perovskite in the laser-heated diamond cell. Eos Trans. AGU 87 (52) Fall Meet. Suppl., Abstract V41D–1763.

Rüpke, L.H., Phipps Morgan, J., Hort, M., Connolly, J.A.D., 2004. Serpentine and the subduction zone water cycle. Earth Planet. Sci. Lett. 223, 17–34.

Sano, A., Ohtani, E., Kubo, T., Funakoshi, K., 2004. In situ X-ray observation of decomposition of hydrous aluminum silicate $AlSiO_3OH$ and aluminum oxide hydroxide δ-AlOOH at high pressure and temperature. J. Phys. Chem. Solids 65, 1547–1554.

Shatskiy, A., Fukui, H., Matsuzaki, T., Yoneda, A., Yamazaki, D., Ito, E., Katsura, T., in press. Growth of large $MgSiO_3$ perovskite single crystals (1 mm): a thermal gradient method at ultra-high pressure, Amer. Mineral.

Skogby, H., 2006. Water in natural mantle minerals I: pyroxenes. In: Keppler, H., Smyth, J.R. (Eds.), Water in Nominally Anhydrous Minerals. Rev. Mineral. Geochem., 62, pp. 155–167.

Smyth, J.R., Frost, D.J., Nestola, F., Holl, C.M., Bromiley, G., 2006. Olivine hydration in the deep upper mantle: effect of temperature and silica activity. Geophys. Res. Lett. 33, L15301. doi:10.1029/2006GL026194.

Smyth, J.R., 2006. Hydrogen in high pressure silicate and oxide mineral structures. In: Keppler, H., Smyth, J.R. (Eds.), Water in Nominally Anhydrous Minerals. Rev. Mineral. Geochem., 62, pp. 85–115.

Smyth, J.R., Swope, R.J., Pawley, A.J., 1995. H in rutile-type compounds: II. Crystal chemistry of Al substitution in H-bearing stishovite. Am. Mineral. 80, 454–456.

Suzuki, A., Ohtani, E., Morishima, H., Kubo, T., Okada, T., Terasaki, H., Kato, T., Kikegawa, T., 2000. In situ determination of the phase boundary between wadsleyite and ringwoodite in Mg_2SiO_4. Geophys. Res. Lett. 27, 803–806.

Withers, A., Essene, E., Zhang, Y., 2003. Rutile/TiO_2II phase equilibria. Contrib. Mineral. Petrol. 145, 199–204.

Xia, Q.K., Sheng, Y.M., Yang, X.Z., Yu, H.M., 2005. Heterogeneity of water in garnet from UHP eclogites, eastern Dabieshan, China. Chem. Geol. 224, 237–246.

Yasuda, A., Fujii, T., Kurita, K., 1994. Melting phase relations of anhydrous mid-oceanic ridge basalts from 3 to 20 GPa: implications for the behaviour of subducted oceanic crust in the mantle. J. Geophys. Res. 99, 9401–9414.